Characterization of perovskite powders made by different synthesis routes

J. Sfeir[1,*], S. Vaucher[2], P. Holtappels[3], U. Vogt[3], H.-J. Schindler[3], J. Van herle[4], E. Suvorova[5], P. Buffat[5], D. Perret[4], N. Xanthopoulos[6], O. Bucheli[1]

[1]HTceramix SA, EPFL, PSE-A, CH-1015 Lausanne; [2]Swiss Federal Laboratories for Materials Testing and Research, EMPA, Feuerwerkstrasse 39, CH-3602 Thun; [3]Swiss Federal Laboratories for Materials Testing and Research, EMPA, Ueberlandstrasse 129, CH-8600 Dübendorf; [4]Swiss Federal Institute of Technology Lausanne, EPFL, STI-ISE-LENI, CH-1015 Lausanne; [5]Swiss Federal Institute of Technology Lausanne, EPFL, SB-CIME, CH-1015 Lausanne; [6]Swiss Federal Institute of Technology Lausanne, EPFL, STI-IMX-LMCH, CH-1015 Lausanne, Switzerland

Abstract

Strontium lanthanum manganite (LSM) and lanthanum ferrite (LSF) perovskite cathode and oxygen membrane materials were synthesized using different techniques: spray pyrolysis, a modified citrate route, oxalate and carbonate co-precipitations. The use of Ca, a cheaper substituent on the *A*-site, was explored along to the substitution of La by Pr. The preparation conditions of these oxides were studied in conjunction with their physical properties. Calcination temperature, composition homogeneity, phase purity, powder size distribution and the ease of fabrication were assessed. The differently sourced powders of the same nominal composition were characterized by *TG/DTA*, *XRD*, *ICP*, *TEM*, *XPS*, *PSD*, and *BET*. The co-precipitation of La, Ca and Fe was also possible using the cyanide route. This complexation method allowed the precipitation of a crystalline phase as evidenced by *XRD*. Among all methods, the cyanide and carbonate co-precipitation allowed the lowest perovskite phase transformation for LSF and LCF, followed by the nitrate (i.e. '*spray pyrolysis*'). All decompositions were observed to proceed concomitantly, with a temperature close to that of the La complex as evidenced by *TG/DTA*. These phase transformation differences affected much the particle size distribution and the surface areas of these materials, the carbonate and the cyanide routes giving rise to very fine powders in the *n*m range. Moreover, *XPS* analysis indicated a high segregation of the *A*-site elements on the surface of the powders, whereas the La/Sr or La/Ca ratios were similar to the measured *ICP* values. *TEM* analyses indicated further uneven composition distributions. These differences are expected to affect the catalytic and electrochemical properties of these materials.

Keywords: powders-chemical preparation, electron microscopy, perovskites, fuel cells, membranes.

1 Introduction

The lanthanide transition-metal oxides are of technological importance for their use in solid oxide fuel cell, catalysis, oxygen membrane reactors and sensors [1-5]. In SOFC, strontium substituted lanthanum manganite (LSM) is commonly used as a high temperature cathode material. Strontium substituted lanthanum ferrite (LSF) is investigated as alternative cathode

[*] To whom correspondence should be addressed. Present address: Swiss Federal Laboratories for Materials Testing and Research, EMPA, Ueberlandstrasse 129, CH-8600 Dübendorf, Switzerland, e-mail: joseph.sfeir@empa.ch

material in medium temperature SOFCs but also as potential oxygen membrane for oxygen and syngas production. These materials are commonly investigated in relation to their electronic, catalytic and electrochemical properties.

Preparation conditions are in many cases responsible for structural differences and thus for the disparity in catalytic [6], electrocatalytic and electrochemical properties of oxides. In this study, we investigate the influence of different fabrication procedures on the final microstructure and composition of these materials for their use as SOFC cathodes or oxygen membrane materials. Calcination conditions, composition homogeneity, phase purity, powder size distribution and the ease of fabrication are considered.

2 Experimental

The different perovskite powders were prepared according to the formula $(La_{1-x}A_x)_yMO_{3-\delta}$ with A = Ca or Sr, and M = Mn or Fe. All chemicals were purchased from Fluka and the precursors were taken from the same batch.

The spray pyrolysis synthesis started from a saturated aqueous nitrate solution [7] sprayed through an ultrasonic nozzle into a reactor vessel held at 550°C. At the end of the process the furnace was raised to 700°C for 6h in order to ensure complete decomposition of the precursors and initiate the perovskite phase formation. The powders thus obtained were homogenized by ball-milling and then calcined at 1450°C for 2h. Subsequently, further processing steps (ball-milling for 150 h and sieving) were added to obtain the desired powder characteristics.

Citrate gelling was made following the procedure presented by A. Douy [8]. The ligand (L) concentration was set to 1 M and adjusted to $M^{n+}L_n$ (M^{n+}, reacting metal). The pH was set to 6 with NH_4OH 25%. The aqueous solution thus obtained was then evaporated up to 90°C under vacuum and the subsequent gel dried at 100°C and decomposed at 200°C.

For oxalate precipitation, the procedure optimized by J. Van herle et al. [9] for the fabrication of ceria-based powders was implemented. Corresponding solutions of oxalic acid and nitrates were made with concentrations of 0.05, 0.1, 1 and 3 M. For oxalic acid concentrations above 1 M, heating of the media was necessary. In aqueous media, the pH was controlled between 1 and 7, using NH_4OH 25%.

The carbonate precipitations were obtained following a modified route using $(NH_4)_2CO_3$ [10,11]. For that purpose, an equivalent of $^n/_2$ of CO_3^{--} was taken, n being the valency of the reacting metal (M^{n+}). Various pH and metals and carbonate concentrations were studied.

For the cyanide route, potassium $[Fe^{II}(CN)_6]^{4-}$ and $[Fe^{III}(CN)_6]^{3-}$ were used as precipitating agents, based on experiments made by S. Vaucher et al. [12,13] on Co and Cr. The metals concentration was set to 3 M.

A summary of the different powders is given in Table 1. For the oxalate, carbonate and cyanide routes, separate trials were undertaken for each of the elements to determine the appropriate precipitation conditions. All the precipitates were subsequently washed with the solvent followed by isopropanol. Final calcination temperatures were varied. The powders thus obtained were characterized by *TG/DTA*, *XRD*, *TEM-EDS*, *XPS*, *BET*, *PSD* and *ICP*. The *TG/DTA* analyses were performed on a NETZSCH STA 409 cell using an air flow of 50 ml/min and a heating rate of 20°C/min until 1450°C where the samples were held for 30 min.

Electrochemical tests were made following the same procedure described elsewhere [5]. Organic pastes of three differently sourced LSF powders with the same nominal composition were applied as SOFC cathodes on anode supported cells. Tests were made at 800°C in H_2/air.

Table 1: Summary of the *ICP* analyses.

ICP analysis		experimental composition						nominal	%
Label	nominal composition	La	Sr	Mn	Fe	Ca	Pr	sum	sum	deviation
5ULSM73-P	$(La_{0.7}Sr_{0.3})_{0.95}MnO_{3-\delta}$	0.678	0.288	1	0.03	0	0.02	1.966	1.95	100.8
LSF55-P	$La_{0.5}Sr_{0.5}FeO_{3-\delta}$	0.537	0.507	-	1	-	-	2.044	2	102.2
5ULSF73-P	$(La_{0.7}Sr_{0.3})_{0.95}FeO_{3-\delta}$	0.733	0.312	0	1	0	0.02	2.045	1.95	104.9
5ULCF73-P	$(La_{0.7}Ca_{0.3})_{0.95}FeO_{3-\delta}$	0.875	0.01	0.01	1	0.252	0.02	2.127	1.95	109.1
5UPCF73-P	$(Pr_{0.7}Ca_{0.3})_{0.95}FeO_{3-\delta}$	0.01	0	0	1	0.287	0.828	2.115	1.95	108.5
$3ULSM^2/_3{}^1/_3$-Ci	$(La_{0.75}Sr_{0.25})_{0.97}MnO_{3-\delta}$	0.731	0.255	1	-	-	-	1.986	1.97	100.8
5ULSF73-Ci	$(La_{0.7}Sr_{0.3})_{0.95}FeO_{3-\delta}$	0.685	0.277	0	1	0	0.01	1.962	1.95	100.6
LSF37-Ca	$La_{0.3}Sr_{0.7}\ FeO_{3-\delta}$	0.3	0.672	-	1	-	-	1.972	2	98.6
LSF55-Ca	$La_{0.5}Sr_{0.5}FeO_{3-\delta}$	0.505	0.494	-	1	-	-	1.999	2	99.95
5ULSF73-Ca	$(La_{0.7}Sr_{0.3})_{0.95}FeO_{3-\delta}$	0.704	0.283	0	1	0	0.01	1.987	1.95	101.9
LSF73-Ca	$La_{0.7}Sr_{0.3}FeO_{3-\delta}$	0.713	0.295	1	-	-	-	2.008	2	100.4
5OLSF73-Ca	$(La_{0.7}Sr_{0.3})_{1.05}FeO_{3-\delta}$	0.757	0.314	1	-	-	-	2.071	2.05	101.0
5UPSF73-Ca	$(Pr_{0.7}Sr_{0.3})_{0.95}FeO_{3-\delta}$	-	0.278	1	-	-	0.851	2.129	1.95	109.2

The prefix and suffix stand for: U:under-stoichiometric, O: over-stoichiometric, P:*'spray pyrolysis'*, Ci: citrate, Ca: carbonate. The error on Fe detection is of about 0.03.

3 Results and discussion

Optimal coprecipitation conditions

For the oxalate, the optimal precipitation conditions within the narrowly modified parameters were identified as: pH ≈ 7, $[M^{n+}]$ = 1M, [L] = 0.5 M. Some leaching was observed for Fe and Mn, independently of the conditions. This is related to the solubility of their oxalates in water ($MnC_2O_4.2H_2O$: 0.037 g / 100 ml; $FeC_2O_4.2H_2O$: 0.022 g / 100 ml; $Fe_2(C_2O_4)_3.5H_2O$: very soluble). Furthermore, Ca, Mn and Sr precipitated well only at a neutral pH.

The carbonate's optimal conditions were identified as: natural pH ≈ 8, $[M^{n+}]$ = 1-3 M, [L] = 0.5-1 M. The $(NH_4)_2CO_3$ concentration had to be set to 0.5 M for high metal concentrations as the solution tended to be very viscous after precipitation. No Fe leaching was observed (no coloration upon KSCN addition).

In the case of the cyanide, the metal concentration was set to 3M. Sr substituted $LaFeO_3$ could not be synthesized as Sr did not precipitate as observed by cross reactions between Sr nitrate and $[Fe^{II}(CN)_6]^{4-}$ or $[Fe^{III}(CN)_6]^{3-}$. For Ca, precipitation was only observed with $[Fe^{II}(CN)_6]^{4-}$. Thus, Ca-substituted $LaFeO_3$ was the only powder produced following this procedure. Interestingly, to our knowledge, this is the first reported cyanide precipitation relating La, Ca and Fe, as previous works in this field are based on the binary $LaFeO_3$, with $[Fe^{III}(CN)_6]^{3-}$ as precursor [14,15]. The results will be reported in more details elsewhere.

Powder characterization

From *TG/DTA* analyses on precipitates, the carbonates were observed to allow first the perovskite transformation at a temperature of 650°C. The observed trend was as follows:

$$LSF_{carbonate}\,650°C < LSF_{nitrate}\,660°C < LSF_{citrate}\,680°C < LSF_{oxalate}\,800°C$$

$$LCF_{carbonate}\,650°C < LCF_{cyanide}\,670°C < LCF_{oxalate}\,700°C < LCF_{citrate}\,900°C$$

All decompositions were observed to proceed concomitantly, with a temperature close to that of the La complex (see Fig.1 for the nitrate, i.e. '*spray pyrolysis*'). For the carbonate precipitates containing Fe, the iron moiety is thought to exist as a hydroxy rather than a carboxy group as no Fe^{III} carbonate could be found in literature.

All co-precipitated powders were amorphous before calcination, except for the LCF precursor made by the cyanide route, in which the precipitation of a nanocrystalline hexacyano complexe occurred (see Fig.2). *XRD* analyses were also performed on powders calcined at different temperatures, mainly at 900, 1000 and 1100°C. In the case of oxalate powders, *XRD*-phase purity was only reached after sintering at 1100°C. This was also the case for the LCF and LSM obtained from carbonates. For the cyanide, a phase transformation to the perovskite structure is observed at 450°C in which the cyanide ligands in the hexacyano-precipitate are replaced by oxygen (Fig.2). For the $La_{1-x}Sr_xFeO_3$ made from carbonates, *XRD*-phase purity was already reached at 800°C (see Fig.3) in contrast to '*spray pyrolysis*' where higher thermal treatments (1200°C) were needed.

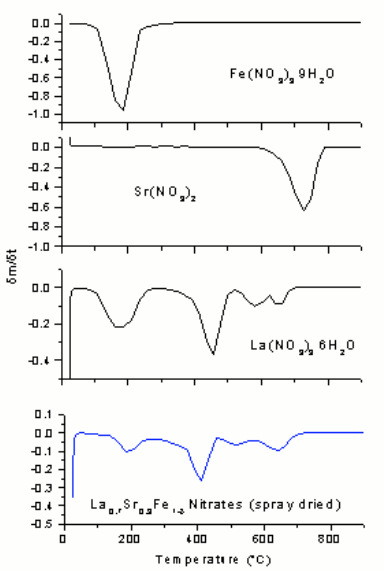

Fig.1: *TG/DTA* analysis of the decomposition of pure Fe, Sr, and La nitrates compared to the spray dried LSF nitrate mixture. The decomposition feature of the mixture resembles that of La. It is clearly seen that the Sr peak disappears.

ICP elemental composition analyses (Table 1) indicated that all powders were, within a max of 4%, near the nominal values with the exception of the Pr perovskites (probably due to uncertainty in the Pr precursor content).

TEM-EDS measurements were done on a dozen of particles of 10 – 200 *n*m. Preliminary analysis shows large scattering in the Sr or Ca content among these particles. For 5ULSM73-P, the generic formula was $La_{1-x}Sr_xMnO_m$, with $0.02 \leq x \leq 0.44$. For 5ULSF73-P, the Sr content varied with $0.04 \leq x \leq 0.24$. With 5ULCF73-P, the *EDS* analysis suggests the generic formula $(La_{1-x}Ca_x)_{0.54}Fe_{0.46}O_m$, with $0.1 \leq x \leq 0.3$. For the 5ULSF73-Ci, an estimated $(La+Sr)_7Fe_3O_m$ formula was obtained. The Sr content varied as $0.01 \leq x \leq 0.36$. From diffraction patterns many phases were present.

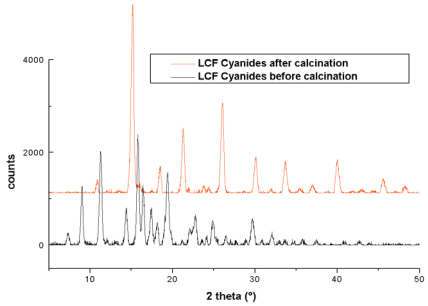

Fig.2 : *XRD* pattern for the LCF-cyanide before and after calcination of the cyanide precursor. A crystalline structure is observed for the hexacyano complex.

For the phases containing the 3 metal elements, $La_2SrFe_2O_7$ and $(La_{1-x}Sr_x)FeO_3$, identified the closest this composition. In the case of 5ULSF73-Ca a generic formula of $(La_{1-x}Sr_x)FeO_m$ with $0.16 \leq x \leq 0.34$ was obtained and the powder corresponded well to the $LaFeO_3$ phase with different Sr content. 5UPCF73-P contained multiple phases. By *EDS* and diffraction, some areas indicated the presence of a Pr rich oxide, lacking Fe and Ca, and related to the $Pr_2O_{7,trigonal}$ phase. The generic formula obtained was $Pr_{1-x}Ca_xFeO_m$, with $0.04 \leq x \leq 0.24$.

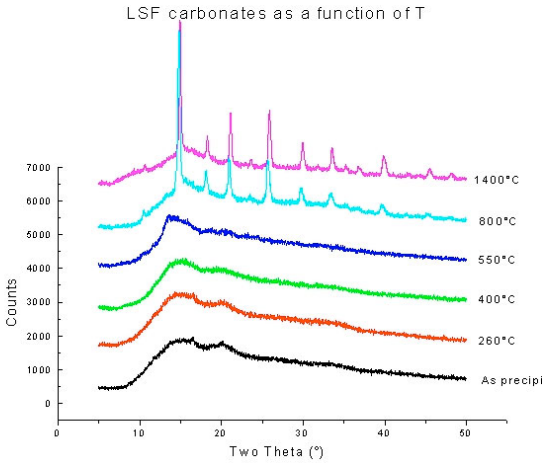

Fig.3: *XRD* patterns of 5ULSF73-Ca carbonate taken after different sintering temperatures. The LSF is seen to change to a perovskite structure after calcination at 800°C.

In all these cases the nominal value for x would have been of 0.285. These nano-scale discrepancies occur independently of the fabrication route and the *XRD* purity. Statistical analyses would be needed to confirm these results but also to get a clear idea on the scattering caused by the different methods. This work is on- going.Globally, from this qualitative analysis, 5ULSF73-Ca is observed to show a more homogeneous Sr distribution than in the cases of 5ULSF73-Ci and 5ULSF73-P.

Table2: Powder size distribution and *BET* values.

Powder	*PSD* (d_{50}) [µm]	*BET* [m^2/g]	remark
5ULSM73-P	0.387		bimodal
5ULSF73-P	0.504	15.4	bimodal
5ULCF73-P	0.459		bimodal
5ULSF73-Ci	1-2	3.82	wide range
3ULSM$^2/_3{}^1/_3$-Ci	1-2	3.73	wide range
5ULSF73-Ca	0.1	8.04	*SEM/TEM*

Table 3: Summary of the *XPS* surface analyses given in percent.

XPS analysis	ratio							
Powder	Mn/La+Sr	Fe/La+Sr	Fe/La+Ca	Fe/Pr+Ca	La/Sr	La/Ca	Pr/Ca	*XPS* composition
5ULSM73-P	38/62				71/29			$(La_{0.71}Sr_{0.29})_{0.62}Mn_{0.38}$
5ULSF73-P		32/68			70/30			$(La_{0.70}Sr_{0.30})_{0.68}Fe_{0.32}$
5ULCF73-P			31/69			71/29		$(La_{0.69}Ca_{0.31})_{0.71}Fe_{0.31}$
5UPCF73-P				25/75			74/26	$(Pr_{0.74}Ca_{026})_{0.75}Fe_{0.25}$
5ULSF73-Ci.		45/56			57/44			$(La_{0.57}Sr_{0.44})_{0.68}Fe_{0.32}$
5ULSF73-Ca		36/64			63/37			$(La_{0.63}Sr_{0.37})_{0.64}Fe_{0.36}$

Furthermore, *XPS* measurements showed differential segregation on the surface of these powders with a much higher ratio for the *A*-site elements (Table 2). Such a high *A*-site concentration is also observed on other perovskite powders [3,16,17] and is thought to influence the catalytic activities due to differences in the number of active reaction sites. Among all powders, a much higher Sr content was observed for 5ULSF73-Ci and 3ULSM$^{2}/_{3}{}^{1}/_{3}$-Ci.

PSD and *BET* analyses (Table 3) made on some of the samples show that citrate powders had much coarser particles probably due to the short milling step (24 h). Coarse '*spray pyrolysis*' powders sintered at 1400°C were brought to a much finer structure upon intensive milling (≈150 h). 5ULSF73-P shows a large surface area indicating the presence of mesoporous agglomerates. LSF-carbonates, on the other hand, showed the finest structure after sintering at 900°C (see Fig.4).

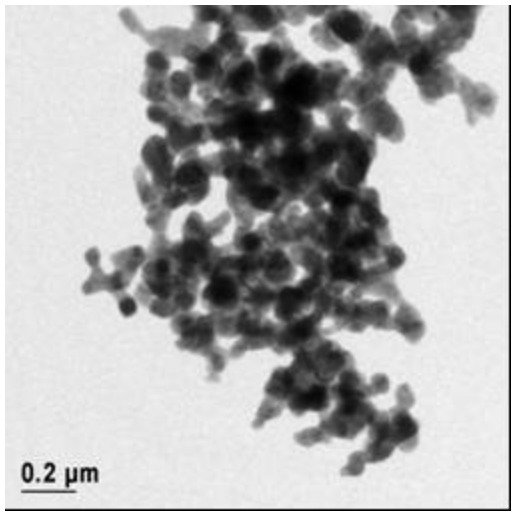

Fig.4: *TEM* micrograph of 5ULSF73-Ca calcined at 900°C.

Globally, these results indicate the possible implementation of carbonate co-precipitation as an alternative method for the synthesis of LSM and LSF on a large scale. A preliminary study made on a semi-pilot installation using static mixers and pumps showed the feasibility of this approach. A few hundreds of grams were produced easily in 5 min time.

Influence of the fabrication route on the electrochemical performance

Preliminary electrochemical measurements made at 800°C on 5ULSF73-Ci, 5ULSF73-Ca and 5ULSF73-P based cathodes having the same nominal composition presented discrepancies in their behaviour (Fig.5). The 5ULSF73-Ci cathode performed poorly when compared to the other two.

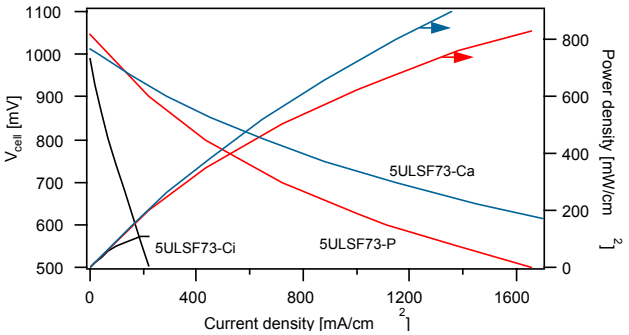

Fig.5: Electrochemical characterization at 800°C of 5ULSF73-P, 5ULSF73-Ci and 5ULSF73-Ca SOFC cathodes deposited on a thin anode supported electrolyte and sintered at 1100°C/4h. The electrolyte thickness was of 5 μm. The cathode and the cell areas were of 1 cm^2 and 16 cm^2 respectively. Air and wet H_2 were used at the cathode and anode respectively.

These results might be understood in light of the disparities in the morphology (*PSD* and *BET*) and/or powder characteristics (*TEM*, *XPS* and *ICP*) reported above. Electrochemical simulations predict a significant enhancement of performance for well structured mixed ionic- electronic cathodes [18]. The geometry dependence of the polarization resistance is considerably influenced by the ratio $^{k}/_{D}$. This value is of

about 30 to 270 for LSF and 10^5 to 10^6 for LSM [19,20]. The nanostructured 5ULSF73-Ca and 5ULSF73-P (*PSD* of 100-500 *n*m) performed much better than the coarse 5ULSF73-Ci (*PSD* 1-2 μm), in agreement with the model. The outer layer composition of the powders might also influence the cathode performance as the surface is the site of the oxygen reduction reaction. These consideration are also true for oxygen membrane materials [21]. However, further studies are needed to clarify these dependencies.

Conclusions

Strontium lanthanum manganite and ferrite were produced by different techniques: '*spray pyrolysis*', a modified citrate route, oxalate, carbonate and cyanide co-precipitation. The influence of the different fabrication procedures on the final microstructure and composition of these materials were investigated. Powders were characterized by *TG/DTA*, *XRD*, *ICP*, *TEM*, *XPS*, *PSD* and *BET*.

'*Spray pyrolysis*' produced mesoporous agglomerates after intensive ball-milling. Powders with a d_{50} = 500 *n*m were thus obtained.

The carbonate route was observed to deliver a finer powder with a more homogeneous composition (100 *n*m, *TEM*). These results indicate the possible implementation of carbonate co-precipitation as an alternative route for the synthesis of lanthanide ferrite and manganite. A semi-pilot installation made using static mixers showed the feasibility of this approach.

The co-precipitation of La, Ca and Fe was also possible using the cyanide route giving rise to a crystalline complex. This is to our knowledge the first reported cyanide precipitation relating La, Ca, and Fe using $[Fe^{II}(CN)_6]^{4-}$.

ICP analyses on all samples showed slight fluctuations between the differently sourced powders. However, due to distinct synthesis routes, sintering temperatures and processing steps morphological differences were observed (*TEM*, *XPS*, *BET* and *PSD*).

As expected, the microstructure and surface composition of these powders triggered disparities in their electrochemical response (SOFC cathode tests). The relative importance of each of these properties is not very clear yet.

Acknowledgements

This work was financed under the TNS 5991.1/6555.1 contract by the Swiss Confederation.

References

1. Gellings, P. J. & Bouwmeester, H. J. M., Solid state aspects of oxidation catalysis. *Catalysis Today*, 2000, **58**, 1-53.
2. Gellings, P. J. & Bouwmeester, H. J. M., Ion and mixed conducting oxides as catalysts. *Catalysis Today*, 1992, **12**, 1-105.
3. Sfeir, J. et al., Lanthanum Chromite Based Catalysts for Oxidation of Methane Directly on SOFC Anodes. *Journal of Catalysis*, 2001, **202**, 229-244.

4. Middleton, H. et al., Co-casting and co-sintering of porous MgO support plates with thin dense perovskite layers of $LaSrFeCoO_3$. *Journal of the European Ceramic Society*, 2004, **24**, 1083-1086.
5. Sfeir, J., Van herle, J. & Vasquez, R., $LaCrO_3$-based anodes for methane oxidation. In *Fifth European Solid Oxide Fuel Cell Forum*, ed. J. Huijsmans, Lucerne, Switzerland, 2002, pp. 570-577.
6. Bell, R. J., Millar, G. J. & Drennan, J., Influence of synthesis route on the catalytic properties of $La_{1-x}Sr_xMnO_3$. *Solid State Ionics*, 2000, **131**, 211-220.
7. Holtappels, P., Vogt, U., Schindler, H. & Gut, B., Perovskite Synthesis by Spray Pyrolysis. In *Fifth European Solid Oxide Fuel Cell Forum*, ed. J. Huijsmans, Lucerne, Switzerland, 2002, pp. 103-107.
8. Douy, A., Polyacrylamide gel: an efficient tool for easy synthesis of multicomponent oxide precursors of ceramics and glasses. *Internaltional Journal of Inorganic Materials*, 2001, **3**, 699-707.
9. Van herle, J. et al,. Sintering behaviour and ionic conductivity of yttria-doped ceria. *Journal of the European Ceramic Society*, 1996, **16**, 961-973.
10. Li, G.-J., Huang, X.-X., Guo, J.-K. & Chen, D.-M., Ni-coated Al_2O_3 powders. *Ceramic International*, 2002, **28**, 623-626.
11. Tanaka, J., Takahashi, K., Yajima, Y. & Tsukioka, M., Lattice constants of monoclinic $(La_{0.8}Ca_{0.2})MnO_3$. *Chemistry Letters*, 1982, 1847-1850.
12. Vaucher, S., Dujardin, E., Lebeau, B., Hall, S. & Mann, S., Higher order construction of molecule-based magnets. *Chemical Materials*, 2001, **13**, 4408-4410.
13. Vaucher, S., Fielden, J., Li, M., Dujardin, E. & Mann, S., Molecule-based magnetic nanoparticles: synthesis of cobalt hexacyanoferrate, cobalt pentacyanonitrosylferrate, and chromium hexacyanochromate coordination polymer in water-in-oil microemulsions. *Nano Letters*, 2002, **2**, 225-229.
14. Sadaoka, Y., Traversa, E., Nunziante, P. & Sakamoto, M., Preperation of perovskite-type $LaFe_xCo_{1-x}O_3$ by thermal decomposition of heteronuclear complex, $La[Fe_xCo_{1-x}(CN)_6].nH_2O$ for electroceramic applications. *Journal of Alloys and Compounds*, 1997, **261**, 182-186.
15. Hulliger, F., Landolt, M. & Vetsch, H., Rare-earth ferricyanides and chromicyanides $LnT(CN)_6.nH_2O$. *Journal of Solid State Chemistry*, 1976, **18**, 283-291.
16. Gunasekaran, N., Bakshi, N., Alcock, C. B. & Carberry, J. J., Surface characterization and catalytic properties of perovskite type solid oxide solutions, $La_{0.8}Sr_{0.2}BO_3$ (B=Cr, Mn, Co or Y). *Solid State Ionics*, 1996, **83**, 145-150.
17. Tabata, K., Matsumoto, I. & Kohiki, S., Surface characterization and catalytic properties of $La_{1-x}Sr_xCoO_3$. *Journal of Materials Science*, 1987, **22**, 1882-1886.
18. Fleig, J. & Maier, J., The polarization of mixed conducting SOFC cathodes: effets of surface reaction coefficient, ionic conductivity and geometry. *Journal of the European Ceramic Society*, 2004, **24**, 1343-1347.
19. Ishigaki, T., Yamauchi, S., Kishio, K., Mizusaki, J. & Fueki, K., Diffusion of oxide ion vacancies in perovskite-type oxides. *Journal of Solid State Chemistry*, 1988, **73**, 179-187.
20. Adler, S. B., Lane, J. A. & Steele, B. C. H., Electrode kinetics of porous mixed-conducting oxygen electrodes. *Journal of the Electrochemical Society*, 1996, **143**, 3554-3564.
21. Diethelm, S., Van herle, J., Sfeir, J. & Buffat, P., Correlation between oxygen transport properties and microstructure in $La_{0.5}Sr_{0.5}FeO_{3-\delta}$. Submitted to the *Journal of the European Ceramic Society*.